

# Spatially-guided Temporal Aggregation for Robust Event-RGB Optical Flow Estimation

Qianang Zhou, Junhui Hou, *Senior Member, IEEE*, Meiyi Yang, Yongjian Deng, Youfu Li, *Fellow, IEEE*, Junlin Xiong, *Member, IEEE*

**Abstract**—Current optical flow methods exploit the stable appearance of frame (or RGB) data to establish robust correspondences across time. Event cameras, on the other hand, provide high-temporal-resolution motion cues and excel in challenging scenarios. These complementary characteristics underscore the potential of integrating frame and event data for optical flow estimation. However, most cross-modal approaches fail to fully utilize the complementary advantages, relying instead on simply stacking information. This study introduces a novel approach that uses a spatially dense modality to guide the aggregation of the temporally dense event modality, achieving effective cross-modal fusion. Specifically, we propose an event-enhanced frame representation that preserves the rich texture of frames and the basic structure of events. We use the enhanced representation as the guiding modality and employ events to capture temporally dense motion information. The robust motion features derived from the guiding modality direct the aggregation of motion information from events. To further enhance fusion, we propose a transformer-based module that complements sparse event motion features with spatially rich frame information and enhances global information propagation. Additionally, a mix-fusion encoder is designed to extract comprehensive spatiotemporal contextual features from both modalities. Extensive experiments on the MVSEC and DSEC-Flow datasets demonstrate the effectiveness of our framework. Leveraging the complementary strengths of frames and events, our method achieves leading performance on the DSEC-Flow dataset. Compared to the event-only model, frame guidance improves accuracy by 10%. Furthermore, it outperforms the state-of-the-art fusion-based method with a 4% accuracy gain and a 45% reduction in inference time.

**Index Terms**—event-based vision, optical flow, modal fusion.

## I. INTRODUCTION

**O**PTICAL flow estimation plays a vital role in understanding object motion between image pairs, providing valuable insights into scene dynamics. Frame-based optical flow methods have leveraged the consistent visual appearance of images, leading to extensive development. Over the past decade, learning-based approaches have dominated this field, with correlation-based architectures [1], [2] becoming the predominant paradigm. These methods effectively address large-baseline motion by establishing correlation between all pixel

pairs using stable appearance features from frames. However, optical flow estimation faces significant challenges despite its success in general scenarios. Frame data becomes unreliable in high dynamic range or rapid motion environments, where most frame-based algorithms fail to perform effectively [3].

Event cameras excel in these challenging scenarios, offering high-frequency motion information that opens new opportunities for visual algorithms [3]–[10]. Their unique characteristics facilitate motion estimation across a broader range of scenes, driving advancements in tasks such as motion deblurring [11]–[14], object tracking [15], [16], and video interpolation [17]–[21]. Recently, event-based optical flow algorithms have gained considerable traction. Unlike frames, event data provides exceptional temporal resolution and dynamic range but lacks consistent visual appearance. State-of-the-art methods [22], [23] leverage the high temporal resolution of events to address issues related to spatial sparsity and noise. Although integrating intermediate motion cues has proven to enhance performance, the inherent sparsity of events often results in unstable feature representation. As illustrated in Fig. 1, event-only methods face challenges such as lack of texture, resulting in structural information loss and inconsistent estimates across consecutive frames. These challenges underscore the need for combining frames and events to improve performance.

Given the highly complementary nature of frames and events, various task-specific fusion strategies have been proposed to improve performance [24]. However, fusion-based optical flow algorithms remain relatively underdeveloped, particularly in exploiting the complementary strengths of frames and events. For example, Gehrig et al. [23] combine motion features from both modalities through direct concatenation, without accounting for their distinct characteristics. Wan et al. [25] constructs cross-modal correlation maps but overlooks intra-modality similarities. We argue that it is essential to fully account for the unique properties and complementary strengths of different modalities and to design effective fusion strategies specifically tailored for optical flow estimation.

To this end, we analyze the advantages of the two modalities in optical flow estimation. Frame features exhibit stable visual appearance in most scenarios, enabling robust spatial correspondences. Event features, on the other hand, provide rich temporal information and retain essential visual structures in challenging environments. Moreover, frames are spatially dense but temporally sparse, whereas events exhibit the opposite characteristics. Building on this observation, we propose leveraging frame data to generate robust spatial correspondences and guide the temporal aggregation of event information. On the other hand, we construct temporally dense

Qianang Zhou is with the Department of Automation, University of Science and Technology of China, Anhui 230026, China, and is also with the Department of Computer Science, City University of Hong Kong, Hong Kong (email: qianazhou2-c@my.cityu.edu.hk).

Junhui Hou is with the Department of Computer Science, City University of Hong Kong, Hong Kong (email: jh.hou@cityu.edu.hk)

Youfu Li is with the Department of Mechanical Engineering, City University of Hong Kong, Hong Kong (email: meyfli@cityu.edu.hk)

Yongjian Deng is with the College of Computer Science, Beijing University of Technology, Beijing, China (yjdeng@bjut.edu.cn)

Meiyi Yang and Junlin Xiong are with the Department of Automation, University of Science and Technology of China, Anhui 230026, China (email: ymy1996@mail.ustc.edu.cn; xiong77@ustc.edu.cn)

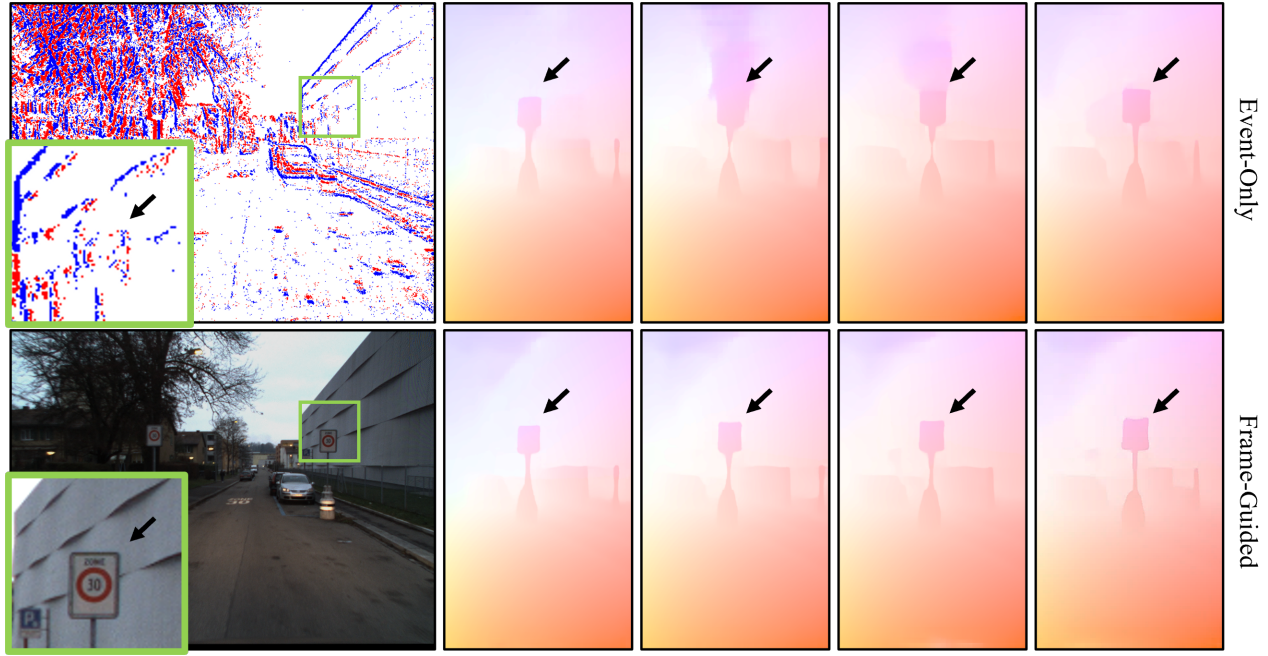


Fig. 1: **Improved prediction stability with frame guidance.** The top row shows results from the event-only method [22], while the bottom row presents results from our method. These four consecutive frames are taken from the `zurich_city_14_c` sequence of DSEC-Flow. The lack of texture information in event data results in unstable predictions. Our method leverages stable frame motion features to guide the aggregation of temporally dense event motion features, leading to consistent predictions across consecutive frames.

correlation maps from event data to extract high temporal resolution motion cues. Our approach integrates the spatial stability of frame data with the temporal richness of event data, enabling effective cross-modal fusion for optical flow estimation.

Specifically, we propose a cross-modal collaborative framework, as depicted in Fig. 2. First, we introduce an event-enhanced frame representation to improve the robustness of the guiding modality. We then extract robust guiding motion features from the frame modality and temporally dense motion features from the event modality. To effectively integrate these features, we design a cross-modal aggregation module, where spatial guiding features supplement sparse event motion features and guide their temporal aggregation. The fused features combine rich spatial information with temporal motion cues, leading to more robust and accurate optical flow predictions. Additionally, we introduce a mix-fusion encoder to extract spatiotemporal context features from both modalities. Our proposed network effectively addresses the instability issues of single-modality methods and achieves substantial improvements over existing fusion approaches, as demonstrated in Fig. 1. Extensive experiments validate the effectiveness of our framework, which achieves state-of-the-art accuracy on the DSEC-Flow [26].

In summary, our primary contributions are as follows.

- We suggest exploiting the advantages of the spatial robustness of frames and the high temporal resolution of events to improve optical flow estimation.
- We propose a novel cross-modal collaboration framework that leverages the reconstructed spatially robust modality

to complement the sparse event features and guide their temporal aggregation.

- We produce state-of-the-art performance on the DSEC-Flow benchmark, i.e., compared to the leading fusion-based methods [23], achieving 4% higher accuracy and 45% faster inference.

The rest of this paper is organized as follows: Sec. II reviews event and frame-based optical flow and cross-modal fusion. Sec. III introduces the preliminaries and event representations used in this study. Sec. IV details the architecture of our framework. Sec. V presents and analyzes the experimental results. Finally, Sec. VI concludes this study.

## II. RELATED WORK

### A. Learning-based Frame Optical Flow

Learning-based methods have emerged as the predominant approach in optical flow estimation in recent years. FlowNet [27] proposes end-to-end optical flow estimation, demonstrating the potential of learning-based methods for the optical flow task. Building upon this, PWC-Net [28] introduced a more efficient architecture by integrating pyramid processing, warping, and cost-volume construction. This approach leverages the pyramid concept to capture diverse motion magnitudes, improving both accuracy and efficiency. Lite-FlowNet [29] maintained high accuracy while significantly reducing the model size and inference time, making it more suitable for real-time applications. Despite their advancements, these methods faced limitations in handling large motions due to their localized correlation computation. RAFT [1]

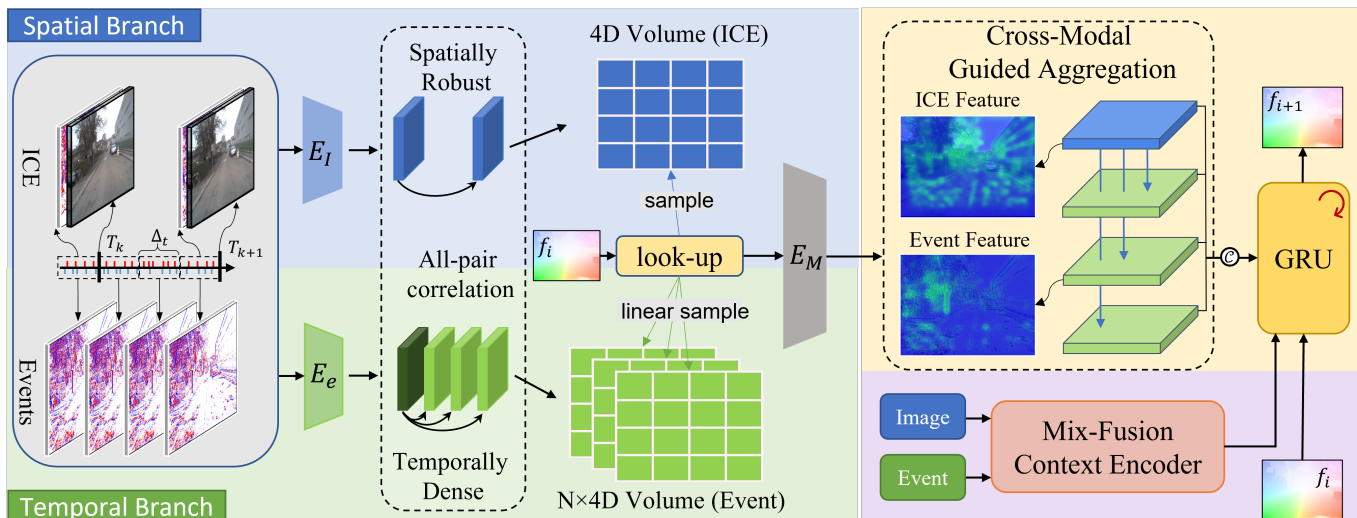


Fig. 2: **The overall architecture of our method.** The core idea of our approach is to leverage the spatial stability of the frame modality to guide the temporal aggregation of event features, enabling complementary interactions between modalities. To achieve this, an event-enhanced frame representation is introduced as robust spatial guidance. Temporally dense motion cues extracted from events are aggregated into strong motion features, and fed into the iterative process. Furthermore, contextual features from both modalities are fused to enhance optical flow estimation.

tackles this challenge by constructing a 4D correlation volume and leveraging diverse non-correlation features for iterative refinement. More recent developments, such as GMFlow [30], reformulate optical flow as a global matching problem based on the 4D correlation volume. Our method is based on the correlation architecture, constructing spatially robust and temporally dense correlation maps within different modalities.

### B. Event-based Optical Flow

Event-based optical flow has seen significant advancements over the past decade. Early approaches [31] fit local planes in the event stream to estimate optical flow, while others [32], [33] minimized an energy function using variational optimization. Shiba et al. [34] warps events along point trajectories, deriving an intuitive flow solution. Recently, learning-based methods have demonstrated distinct advantages. Self-supervised methods [35], [36] primarily use contrast maximization [37] or temporal loss [35] to supervise the learning process, while supervised methods rely on labeled data. Notable examples include EvFlowNet [35] and E-RAFT [26], which successfully adapted FlowNet [27] and RAFT [1] architectures for event data. Based on E-RAFT, TMA [22] further utilizes the high temporal resolution of event data to compensate for spatial sparsity. Recently, TCM [38] introduced multi-scale timestamp loss to supervise dense optical flow prediction, achieving notable success. Moreover, Wan et al. [25] and Gehrig et al. [23] integrated image and event data to estimate dense optical flow. Our method emphasizes leveraging the unique characteristics of each modality and their complementary advantages to enable effective cross-modal collaboration.

### C. Event-Frame Cross-Modal Fusion

The complementary nature of events and frames has been extensively explored in various tasks such as semantic segmentation [24], [39]–[41], depth estimation [42]–[44], and object tracking [45], [46]. In these applications, it is common to employ a multi-stage fusion of event and image features within a UNet-like framework, followed by processing the fused features through the decoder. Chen et al. [46] develop an adaptive sampling method to align event and image modalities, along with a bidirectional-enhanced framework to facilitate cross-modal tracking. Zhu et al. [45] introduce a mask modeling strategy to promote proactive interaction between tokens from different modalities. Several approaches have also explored the integration of events and frames for optical flow estimation. For example, DCEIFlow [25] generates a pseudo-feature for the second frame by fusing the first frame with events and then estimates the optical flow based on the RAFT structure. BFlow [23] concatenates motion features from both images and events into a single representation and then estimates the control point location of the trajectory. Our method guides the aggregation of temporal motion features using spatially robust frame motion features, enabling the fusion of motion cues for optical flow estimation.

## III. PRELIMINARY AND DATA REPRESENTATION

The event and frame data are significantly different and it is necessary to reorganize them. An event is triggered when a pixel of the event camera detects a change in luminance above a threshold  $C$ . Each event  $e_i$  typically includes the time  $t_i$ , coordinates  $(x_i, y_i)$  and the polarity  $p_i$  of its occurrence. The asynchronous events are usually converted into a frame-like



Fig. 3: **Illustration of ICE.** The left side shows the event and image reorganization process, with the image captured at time  $t$ .  $\mathbf{V}_{-2}$ ,  $\mathbf{V}_{-1}$ , and  $\mathbf{V}_0$  represent the three voxels preceding  $t$ . The right side illustrates the overlay of events and frames, demonstrating how their combination enhances spatial robustness.

representation. In this paper, we convert the events set into a voxel grid  $\mathbf{V}$ , as in the previous works [35]:

$$\begin{aligned} t_i^* &= (B-1)(t_i - t_1)/(t_N - t_1), \\ \mathbf{V}(x, y, t) &= \sum_i p_i k_b(x - x_i) k_b(y - y_i) k_b(t - t_i^*), \\ k_b(a) &= \max(0, 1 - |a|), \end{aligned} \quad (1)$$

where  $B$  represents the number of time bins,  $t_i^*$  discretizes  $t_i$  to the  $i$ -th time bin, and  $k_b(a)$  is a bilinear interpolation function.

Different time ranges of events and frame data are required to estimate pixel motion from  $T_k$  to  $T_{k+1}$ . For frames data, we use images  $I_k$  and  $I_{k+1}$ , corresponding to timestamps  $T_k$  and  $T_{k+1}$ . The event data representation is illustrated in Fig. 2. We capture temporally dense motion cues by uniformly partitioning the event stream within the interval  $[T_k, T_{k+1}]$  into a sequence of target segments  $\{\mathbf{V}_1, \mathbf{V}_2, \dots, \mathbf{V}_N\}$ , each with an average time span of  $\Delta_t$ . Then we use the segment from the interval  $[T_k - \Delta_t, T_k]$  as the reference segment  $\mathbf{V}_0$ . Correlations between the reference and targets provide rich temporal motion information for flow estimation.

#### IV. PROPOSED METHOD

To facilitate cross-modal collaboration in optical flow estimation, we leverage spatially robust features to guide the temporal aggregation of sparse event features. Sec. IV-A introduces an event-enhanced frame representation to improve the robustness of guidance, and discusses spatial and temporal motion feature extraction. Sec. IV-B details how robust spatial features guide the aggregation of temporally dense event features and our proposed spatiotemporal context feature.

##### A. Spatial Guidance and Temporal Features Construction.

As shown in Fig. 2, we extract spatially robust correlation features in the spatial branch and temporally dense motion

cues in the temporal branch. Building on the data representations outlined in Sec. III, each branch is detailed as follows.

**Robust Spatial Guidance.** Correlation-based methods establish reliable pixel correspondences between two viewpoints to extract motion features. However, high-temporal-resolution event data are often sparse and noisy, complicating accurate optical flow estimation. To address this, we use robust frame features to guide the aggregation of temporally dense event motion features. Frames are susceptible to disturbances like illumination changes and motion blur, so we enhance frame data with events to improve guidance stability. Although events are typically used to enhance frame quality, we introduce a simplified representation called Image-Event Connection (ICE) that avoids complex networks [17] for reconstructing high-quality images. As illustrated in Fig. 3, ICE systematically organizes events and frames, ensuring robust guidance across diverse environments.

Specifically, given the input event voxel  $\mathbf{V}$  and image  $\mathbf{I}$ , we first mapped pixel values and voxel values to  $[-1, 1]$  to balance the contributions of events and frames:

$$\begin{aligned} \hat{\mathbf{I}} &= 2 \times \frac{\mathbf{I}}{255} - 1, \\ \hat{\mathbf{V}} &= \frac{\mathbf{V}}{\max(|\mathbf{V}|) + \epsilon}, \end{aligned} \quad (2)$$

where  $\epsilon$  is a small positive constant to prevent the maximum value from being zero. The ICE is then generated as:

$$\mathbf{ICE} = \text{concat}(\hat{\mathbf{V}}_{t-\Delta_t}^t, \hat{\mathbf{I}}_t), \quad (3)$$

where  $\mathbf{I}_t$  corresponds to time  $t$ , and  $\mathbf{V}_{t-\Delta_t}^t$  represents the voxel from  $t - \Delta_t$  to  $t$ .

As shown in Fig. 3, ICE combines intensity information from images with structural information from events. In low-light conditions, frame data may degrade significantly, while event data still provide sufficient spatial information. In well-lit scenes, frame intensity information complements the event data. Consequently, the motion features extracted from ICE

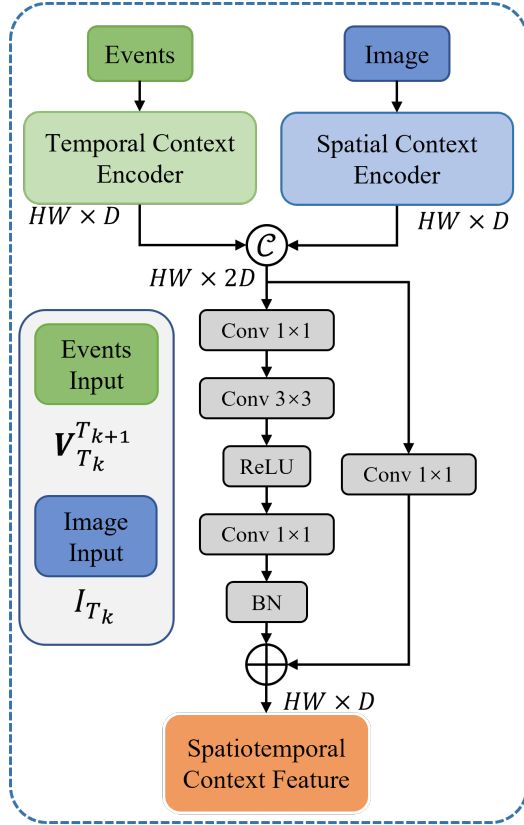


Fig. 4: The architecture of the Mix Fusion Context Encoder. We extract temporal and spatial contextual features from events and images, respectively, and fuse them into spatiotemporal features. Spatial context is extracted from the first frame  $I_k$ , while temporal context includes all events from  $T_k$  to  $T_{k+1}$ .

exhibit high spatial stability, ensuring robust guidance. Note that we use events only within a time window of length  $\Delta t$  to avoid edge blurring caused by long windows.

Subsequently, we extract features from ICE pairs and generate all-pairs correlation volume  $\mathbf{C}_g$  between them for guidance:

$$\mathbf{C}_g = \frac{\mathbf{F}_1 \mathbf{F}_2}{\sqrt{D}}, \quad (4)$$

where feature  $\mathbf{F}_1$  corresponding to the first ICE, and  $D$  is the feature channels. We emphasize that  $\mathbf{C}_g \in \mathbb{R}^{HW \times HW}$  encompasses not only the motion information for the entire optical flow from  $T_k$  to  $T_{k+1}$  but also the robust spatial correlation generated from the ICE, thereby supporting the guidance for event features.

**Temporally Dense Correlation.** The effectiveness of leveraging the high temporal resolution of event data to compensate for extreme sparsity and noise has been validated in several works. TMA [22] and BFlow [23] propose to replace the single correlation volume with temporally-dense correlation volumes and achieved excellent accuracy. Thus we extract event motion cues at multiple intermediate times, following these works.

Specifically, we first split the event stream into a reference  $\mathbf{V}_0$  and a series of targets  $\{\mathbf{V}_n, n \in [1, N]\}$ , as described in Sec. III. The reference  $\mathbf{V}_0$  and the final target  $\mathbf{V}_N$  are aligned

with the first and second frames  $I_k$  and  $I_{k+1}$ , respectively. To ensure consistency, all the targets and the reference share the same feature encoder. The correlation volumes are then generated between the reference and each target, to construct the temporally dense cost volumes:

$$\mathbf{C}_T = \left\{ \frac{\mathbf{F}_{\mathbf{V}_0} \mathbf{F}_{\mathbf{V}_n}}{\sqrt{D}} \right\}, n \in [1, N], \quad (5)$$

where  $\mathbf{F}_{\mathbf{V}_n}$  is the  $n$ -th feature of events and  $D$  is the feature channels.

Cost volumes  $\mathbf{C}_T$  contain motion information with high temporal resolution, yet they are spatially sparse and unstable. Previous work [23] adopted an overlapping strategy to mitigate the adverse effects of sparsity, which sacrifices efficiency and becomes unnecessary with the introduction of frames. The features in  $\mathbf{C}_T$  lack full optical flow information and scene texture, which are precisely what  $\mathbf{C}_g$  contains. Consequently, the motion feature extracted from  $\mathbf{C}_g$  will be used to guide the aggregation of temporal event features from  $\mathbf{C}_T$  in the following.

### B. Context Fusion and Guided Aggregation

**Spatiotemporal Context.** The context encoder extracts features from event or image data to guide optical flow estimation. Spatial context features from frames capture the spatial structural details of  $I_k$ , while temporal context features from events encode information spanning from  $T_k$  to  $T_{k+1}$ . Previous studies have shown that both features enhance optical flow prediction [22], [23], [25], [26]. However, the interplay between spatial and temporal features, as well as their individual contributions, remains unexplored. We argue that combining spatial and temporal contexts yields richer, more informative representations. This paper introduces spatiotemporal context features as a replacement for single-modal features, with further analysis presented in the experimental section.

To achieve this, we propose the Mix-Fusion Context Encoder, illustrated in Fig. 4, to extract spatiotemporal context features from events and frames. We first extract spatial context features from  $I_k$  and temporal context features from  $\mathbf{V}_{T_k}^{T_{k+1}}$  using two separate encoders. Both features are designed to have the same channel dimensions and are subsequently fed into the mix-fusion block. The mix-fusion module is inspired by [47], and the output spatiotemporal feature  $\mathbf{F}_{st}$  has the same number of channels as single-modal context features:

$$\begin{aligned} \mathbf{H} &= \text{concat}(\mathbf{F}_s, \mathbf{F}_t), \\ \mathbf{F}_{st} &= \text{MLP}(\text{Conv}_{3 \times 3}(\text{MLP}(\mathbf{H})) + \text{MLP}(\mathbf{H})), \end{aligned} \quad (6)$$

where  $\text{MLP}(\cdot)$  performs per-pixel feature fusion, and  $\text{Conv}_{3 \times 3}(\cdot)$  is used for local information propagation.

**Cross-Modal Guided Aggregation.** We have generated spatially robust ICE correlation volumes and temporally dense event correlation volumes. In the update branch, ICE motion features guide the temporal aggregation of event features, iteratively refining the optical flow estimation with the aid of spatiotemporal context features.

Correlation-based methods sample the cost map corresponding to the current estimation from the correlation volume,

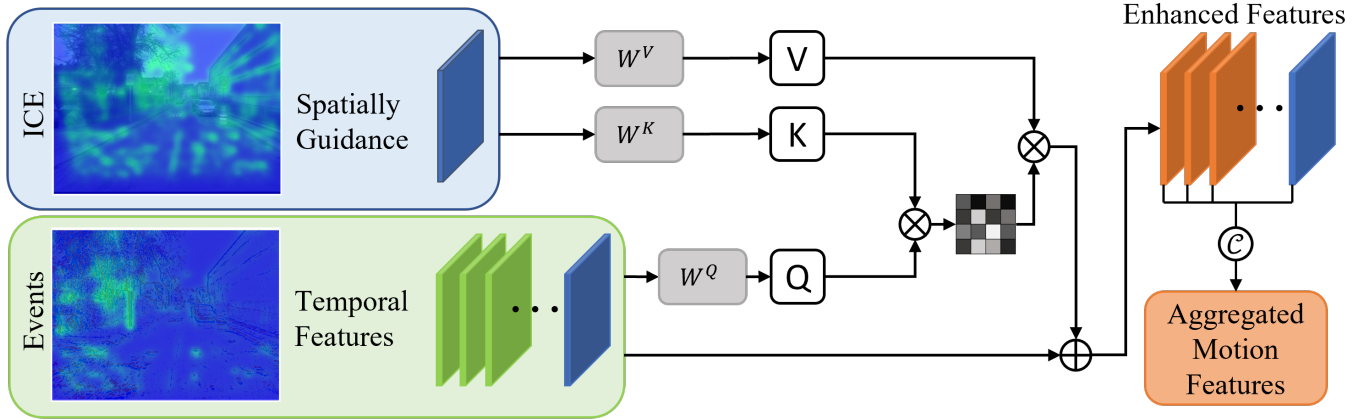


Fig. 5: Illustration of the transformer-based cross-modal guided aggregation strategy. The robust ICE feature (blue) is used as the Key to guide the aggregation of temporally dense event features (green) and also serves as the Value to enhance the spatially sparse event features.

encoding it as motion features to drive further refinement. Our cross-modal approach samples from both modalities using the lookup operation. For the ICE modality, given the current optical flow estimate  $\hat{f}$ , the cost map of  $\hat{f}$  is sampled as:

$$Cost = \text{lookup}(C_g, \hat{f}),$$

where  $\text{lookup}(\cdot, \cdot)$  samples the similarity between pixel pairs from  $C_g$  based on  $\hat{f}$ . For the events modality, each reference-target pair has different time intervals, necessitating a linear lookup strategy [22]. Given the flow estimation  $\hat{f}$ , the  $i$ -th cost map is sampled as:

$$Cost = \text{lookup}(C_T^i, \hat{f}^i), i \in [1, N],$$

where  $C_T^i$  is the  $i$ -th correlation maps in  $C_T$ .

The sampled cost maps are encoded as motion features by  $E_M$ , as shown in Fig. 2. The ICE motion feature  $M_{ice}$  encodes robust visual information, while the event motion features  $\{M_{ev}^i, i \in [1, N]\}$  provide temporally detailed motion cues. Subsequently, we use  $M_{ice}$  to guide the aggregation of  $M_{ev}$ . Inspired by [2], [22], we adopt a transformer to implement the cross-modal guided aggregation:

$$\begin{aligned} Q_{ev}^i &= M_{ev}^i W^Q, \quad Q_{img} = M_{ice} W^Q, \\ K &= M_{ice} W^K, \\ V &= M_{ice} W^V, \end{aligned} \quad (7)$$

$$AM = M + \text{ffn}(\text{softmax}(\frac{QK}{\sqrt{D}})V),$$

where  $D$  is the dimension of  $K$ , and  $\text{ffn}(\cdot)$  is the feed-forward neural network. The  $M_{ice}$  functions as both the Key and the Value, guiding the aggregation of temporal event features and compensating for spatial sparsity in the event data. Eventually, the aggregated features are concatenated into a single motion feature, which is fed into the ConGRU for further refinement.

### C. Supervision

We follow the standard setup of correlation-based methods to supervise the network output. The  $L_1$  distance between the

predictions and the ground truth is taken as the loss, and the supervision is performed on each output of the iterator:

$$\mathcal{L} = \sum_{j=1}^n \gamma^{n-j} \|\hat{f}_j - f_{gt}\|_1,$$

where  $n$  is the total number of ConGRU iterations,  $\hat{f}_j$  is the output of the  $j$ -th iteration, and  $\gamma$  is the decay factor.

## V. EXPERIMENTS

### A. Datasets and Setup

To ensure fair comparisons with prior methods, we conducted extensive experiments on MVSEC [48] and DSEC-Flow [49]. Both datasets provide frame and event data from real-world scenes and are widely adopted for evaluating event-based optical flow. MVSEC includes one daytime outdoor driving sequence, one nighttime outdoor driving sequence, and four indoor flying sequences. We adhered to the same experimental setup as in previous work [35]. Specifically, Experiments on MVSEC were performed at different time intervals,  $dt = 1$  and  $dt = 4$  images. For data partitioning, *outdoor\_day\_2* was used for training, while *outdoor\_day\_1* and three indoor sequences formed the test set. Consistent with prior methods [35], only 800 frames from *outdoor\_day\_1* were used for evaluation.

DSEC-Flow covers a broader range of driving scenarios, including challenging conditions such as nighttime, sunrise, sunset, and tunnels. The dataset provides an official training set and a public online benchmark. The test set of DSEC-Flow also contains various challenging scenes, making it a widely used benchmark for evaluating event-based algorithms. In line with previous studies, we submitted our results to its public benchmark for evaluation.

**Metrics.** The primary accuracy metric for both DSEC-Flow and MVSEC is End-Point-Error (EPE). DSEC-Flow additionally reports Angular Error (AE) and the percentage of EPE exceeding  $N$  pixels (NPE). For MVSEC, we followed prior work to compute outliers, defined as predictions with an

EPE greater than 3 pixels or more than 5% of the ground truth magnitude.

**Train details.** The proposed method was implemented using PyTorch. For event voxelization, following previous methods [22], [26], events between two frames were divided into 15 bins. The number of targets  $N$  was set to 5, resulting in  $\Delta t = 0.2(T_{k+1} - T_k)$ . Consequently, the voxel grid  $V_{T_k - \Delta t}^{T_{k+1}}$  consists of 18 bins, including one reference and five targets. The voxel normalization parameter  $\epsilon$  in ICE was set to 0.1. The search radius for all correlation volumes was set to 4. The decay factor  $\gamma$  was set to 0.85. During training, the batch size was set to 6 and the learning rate was 0.0002. The number of iterations was fixed at 6 for both training and testing. The network was trained on DSEC for 200k steps and MVSEC for 100k steps.

### B. Results of the DSEC-Flow Dataset

**Accuracy.** The overall evaluation results on the DSEC-Flow dataset are summarized in Table I, with detailed results for each sequence provided in Table II. Several conclusions can be drawn from these results. The methods are categorized into three groups based on input type: frame-only, event-only, and cross-modal. Both cross-modal methods outperform the state-of-the-art event-based method ECDDP [50], highlighting that incorporating frame data significantly enhances prediction accuracy. The event branches in our method and BFlow are both based on temporally dense correlation volumes, similar to TMA. To evaluate the effectiveness of the proposed fusion strategy, we compare the performance of our method and BFlow against TMA. Our method improves inter-modal interactions by replacing the simple concatenation mechanism in BFlow with cross-modal guided aggregation. Compared to TMA, BFlow reduces the EPE from 0.74 to 0.69, and our method further reduces the EPE to 0.66, with a 10% improvement in accuracy. These results validate the effectiveness of the guided fusion strategy. Qualitative results in Figs. 1 and 6 show that single-modal approaches often struggle with ambiguity in certain regions due to insufficient intensity and texture information. Our proposed cross-modal guidance strategy effectively mitigates this uncertainty, leading to more stable and consistent predictions across consecutive frames.

For reference, we also report the performance of frame-only methods. The DSEC-Flow test set contains numerous low-light scenes, which limits the performance gains of frame-based methods compared to event-based approaches. The results indicate that integrating event data can enhance the accuracy of frame-only methods, particularly in challenging environments. Finally, we compare our method to other cross-modal approaches. Compared to the state-of-the-art cross-modal method BFlow, our approach achieves a 4% reduction in EPE, demonstrating that the proposed fusion strategy retains the strengths of each modality while enhancing cross-modal collaboration. Our method also shows notable improvements over BFlow in the NPE and AE metrics. As shown in Table II, our method maintains consistent performance across different sequences, underscoring its robustness.

TABLE I: **DSEC-Flow evaluation results.** Bold indicates the best accuracy, while underlining indicates the second best. ‘E’ represents events, and ‘I’ represents images. ‘\*’ indicates that the network is pre-trained with synthetic data. ‘↓’ indicates the smaller, the better.

Method	Input	EPE ↓	1PE ↓	2PE ↓	3PE ↓	AE ↓
RAFT [1]	I	0.78	12.40	4.6	2.61	2.44
GMA [2]	I	0.94	12.98	5.08	2.96	2.66
ERAFT [26]	E	0.79	12.74	4.74	2.68	2.85
TMA [22]	E	0.74	10.86	3.97	2.30	2.68
ECDDP [50]	E	0.70	8.89	3.20	1.96	2.58
IDNet [51]	E	0.72	10.07	3.50	2.04	2.72
BFlow [23]	E+I	0.69	9.70	3.42	1.88	2.42
<b>Ours</b>	E+I	<u>0.66</u>	<u>8.58</u>	<u>2.93</u>	<u>1.68</u>	<u>2.37</u>
<b>Ours*</b>	E+I	<b>0.63</b>	<b>7.93</b>	<b>2.61</b>	<b>1.45</b>	<b>2.29</b>

This study also investigates the effect of pretraining with synthetic data [23] on performance. The synthetic dataset, similar to FlyingChairs [27], differs significantly from real-world driving scenarios [26]. The network was initialized with parameters trained on this synthetic dataset, while all other settings unchanged. As shown in Table II, pretraining substantially improves network performance, highlighting the strong potential of synthetic data for enhancing optical flow accuracy.

**Robustness Analysis.** The ICE representation integrates both events and frames, providing robust guidance across diverse scenarios. We validate the robustness of our approach by evaluating it on the DSEC-Flow test set, which contains challenging scenes. The detailed evaluation results are presented in Table II. Since comprehensive results for BFlow are unavailable, we compare our method with TMA [22] and ECDDP [50]. Additionally, Fig. 6 provides a qualitative comparison, showcasing the nighttime sequence *zurich\_city\_12\_a* and the daytime sequence *zurich\_city\_14\_c* as representative examples.

As shown in Table II, our method achieves the highest prediction accuracy across both challenging and regular scenes. By leveraging the texture information from frames, the proposed approach demonstrates significant improvements in regular scenes. For example, our method outperforms TMA by 17% on the *zurich\_city\_14\_c* sequence. The bottom row of Fig. 6 highlights that even in well-lit scenes, events may still lack sufficient texture information, which leads to errors. Our approach addresses this by using stable ICE features to compensate for the sparse event features, substantially improving accuracy. Notably, our method surpasses the state-of-the-art event-based method ECDDP [50] in nighttime scenarios, despite reduced frame quality. For instance, our method achieves a 12% accuracy improvement over ECDDP on the *zurich\_city\_12\_a* sequence. This performance gain likely stems from the tendency of event cameras to generate increased noise in low-light conditions, while prominent edges and illuminated areas in frames still provide valuable information. ICE features enhance the robustness of guiding features by effectively integrating event data. Another demonstration of the robustness of our method is the prediction consistency

TABLE II: **Detail results on DSEC-Flow.** Bold indicates the best accuracy. All results are available on the public online benchmark of DSEC-Flow.

Method	Overall			interlaken_00_b			interlaken_01_a			thun_01_a		
	EPE(↓)	3PE(↓)	AE(↓)	EPE(↓)	3PE(↓)	AE(↓)	EPE(↓)	3PE(↓)	AE(↓)	EPE(↓)	3PE(↓)	AE(↓)
ERAFT [26]	0.79	2.68	2.85	1.39	6.19	2.36	0.90	3.91	2.54	0.65	1.87	2.94
TMA [22]	0.74	2.30	2.68	1.39	5.79	2.157	0.81	3.11	2.23	0.62	1.61	2.88
IDNet [51]	0.70	1.96	2.58	1.25	4.35	2.11	0.77	2.60	2.25	0.57	1.47	2.66
ECDDP [50]	0.72	2.04	2.72	1.31	5.03	2.00	0.76	2.47	2.18	<b>0.52</b>	1.36	<b>2.34</b>
<b>Ours</b>	<b>0.66</b>	<b>1.68</b>	<b>2.37</b>	<b>1.22</b>	<b>4.32</b>	<b>1.96</b>	<b>0.72</b>	<b>2.10</b>	<b>2.06</b>	0.55	<b>1.31</b>	2.43

Method	thun_01_b			zurich_city_12_a			zurich_city_14_c			zurich_city_15_a		
	EPE(↓)	3PE(↓)	AE(↓)	EPE(↓)	3PE(↓)	AE(↓)	EPE(↓)	3PE(↓)	AE(↓)	EPE(↓)	3PE(↓)	AE(↓)
ERAFT [26]	0.58	1.52	2.20	0.61	1.06	4.50	0.71	1.91	3.43	0.59	1.30	2.55
TMA [22]	0.55	1.31	2.10	0.57	0.87	4.38	0.66	1.99	3.09	0.55	1.08	2.51
IDNet [51]	0.55	1.35	2.07	0.60	1.16	4.56	0.76	2.74	3.74	0.55	1.02	2.55
ECDDP [50]	0.51	1.21	1.93	0.55	0.76	4.35	0.69	2.39	3.22	<b>0.52</b>	<b>0.89</b>	2.41
<b>Ours</b>	<b>0.50</b>	<b>1.12</b>	<b>1.76</b>	<b>0.50</b>	<b>0.54</b>	<b>3.80</b>	<b>0.55</b>	<b>0.94</b>	<b>2.47</b>	0.53	0.92	<b>2.27</b>

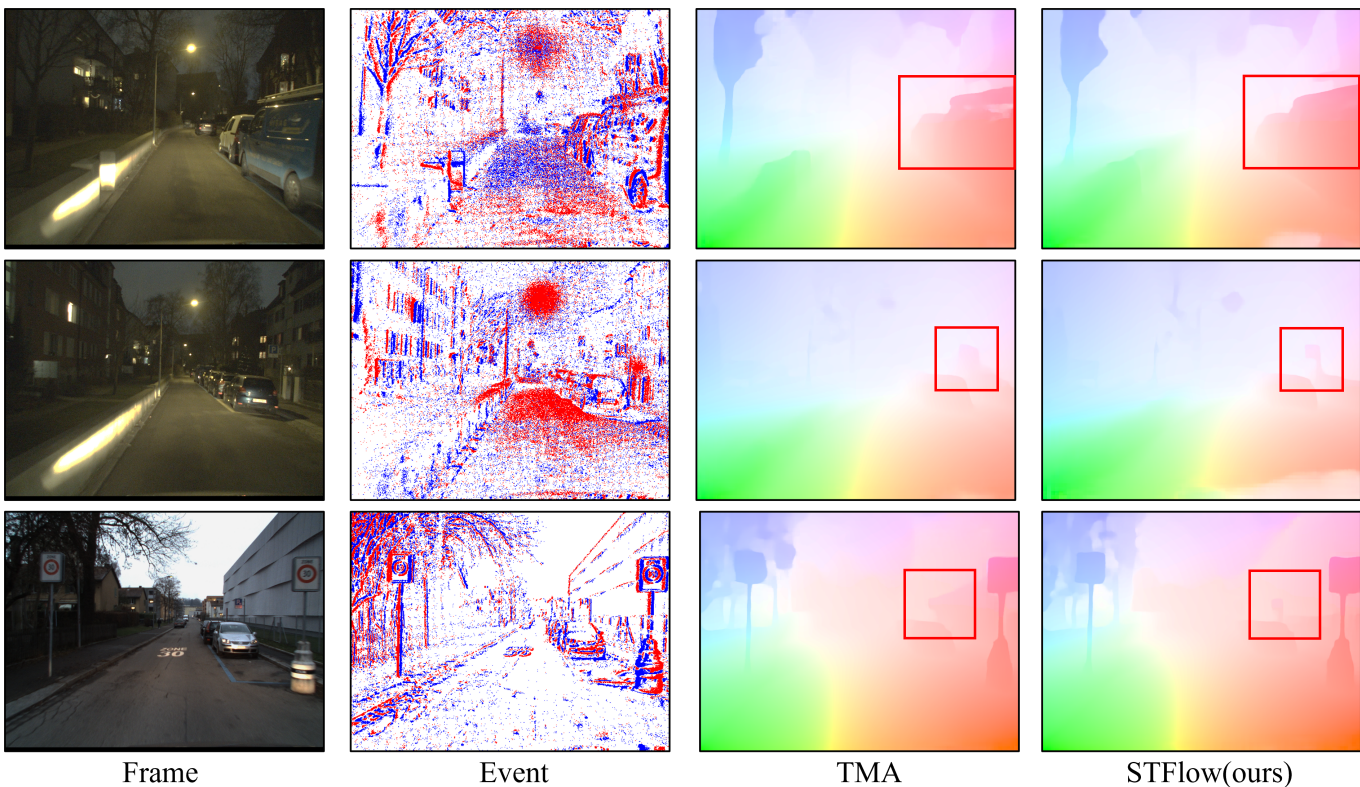


Fig. 6: **Qualitative results on DSEC-Flow.** The first two rows display the night scene *zurich\_city\_12\_a* with contrast-adjusted images for improved visibility. The bottom row shows the daytime scene *zurich\_city\_14\_c*. The third and fourth columns compare the event-only method TMA [22] with our method.

shown in Fig. 1. Our guided fusion strategy ensures stable spatial features, providing a critical advantage over other cross-modal approaches.

### C. Results of the MVSEC Dataset

We evaluated the generalization performance of our method on the MVSEC dataset, as reported in Table III. In accordance with the experimental setup, all models were trained on the *outdoor\_day\_2* sequence and tested on the indoor and *outdoor\_day\_1* sequences. The domain gap between

*outdoor\_day\_1* and *outdoor\_day\_2* is relatively small, while the gap between the indoor sequence and *outdoor\_day\_2* is more substantial. As shown in Table III, our method achieves significantly higher accuracy on the indoor sequence compared to event-only approaches, while performing less effectively on the *outdoor\_day\_1* sequence. These results indicate that our fusion strategy reduces overfitting, thereby improving generalization.



TABLE III: **Evaluation results on MVSEC.** Bold indicates the best accuracy. ‘%Outlier’ denotes the proportion of outliers to all valid pixels.

Method	Input	indoor_flying_1				indoor_flying_2			
		dt=1		dt=4		dt=1		dt=4	
		EPE(↓)	%Outlier(↓)	EPE(↓)	%Outlier(↓)	EPE(↓)	%Outlier(↓)	EPE(↓)	%Outlier(↓)
ERAFT [26]	E	1.10	5.72	2.81	40.25	1.94	30.79	5.09	64.19
TMA [22]	E	1.06	3.63	2.43	29.91	1.81	27.29	4.32	52.74
<b>Ours</b>	E+I	<b>0.89</b>	<b>2.38</b>	<b>2.27</b>	<b>28.03</b>	<b>1.55</b>	<b>18.49</b>	<b>4.16</b>	<b>48.38</b>

Method	Input	indoor_flying_3				outdoor_day_1			
		dt=1		dt=4		dt=1		dt=4	
		EPE(↓)	%Outlier(↓)	EPE(↓)	%Outlier(↓)	EPE(↓)	%Outlier(↓)	EPE(↓)	%Outlier(↓)
ERAFT [26]	E	1.66	25.20	4.46	57.11	<b>0.24</b>	<b>0.00</b>	0.72	1.12
TMA [22]	E	1.58	23.26	3.60	42.02	0.25	0.07	<b>0.70</b>	<b>1.08</b>
<b>Ours</b>	E+I	<b>1.19</b>	<b>13.22</b>	<b>3.01</b>	<b>33.24</b>	0.32	<b>0.00</b>	0.79	2.04

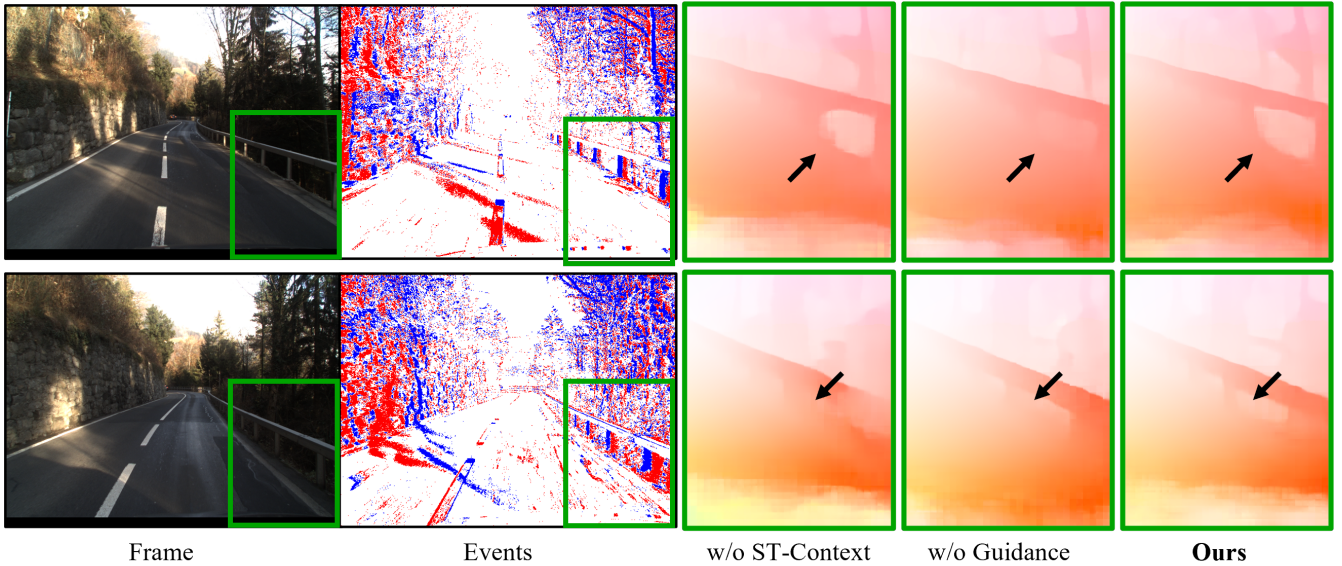


Fig. 7: **Qualitative ablation studies.** When significant overlap occurs between foreground and background events, the network tends to experience regional confusion. Introducing frame data alone does not fully address this issue. Our proposed cross-modal guided aggregation strategy reduces errors by using stable ICE features to guide event features. Additionally, replacing single-modal context with compact spatiotemporal context features leads to notable performance improvements.

D. Ablation Study

We conducted a series of ablation experiments to validate the proposed improvements: Enhanced Representation for Guidance, Spatiotemporal Context, and Cross-Modal Guided Aggregation. All ablation models were trained on DSEC-Flow and evaluated on the DSEC-Flow public benchmark.

**Enhanced Representation for Guidance.** ICE was introduced to enhance the stability of frame features used for guidance. To evaluate its effectiveness, we replaced ICE with standard frames in the optimal configuration and retrained the model. As shown in Table IV, frame guidance leads to a decrease in accuracy compared to ICE. This conclusion aligns with our observations in Fig. 3, indicating that ICE features exhibit more robust spatial structural information. Overall, we conclude that ICE provides more robust guidance than standard frame features.

**Spatiotemporal Context.** We introduce the mix-fusion

TABLE IV: **Ablation study on DSEC-Flow.** Bold text highlights the contributions of this study, where ‘ST’ refers to the spatiotemporal context feature and ‘GA’ represents the guided aggregation strategy.

	Ablation Settings			Metrics		
	Guidance	Context	Fusion	EPE	1PE	3PE
1	Frame	<b>ST</b>	<b>GA</b>	0.67	8.81	1.70
2	<b>ICE</b>	Frame	<b>GA</b>	0.69	9.54	1.79
3	<b>ICE</b>	Events	<b>GA</b>	0.68	8.86	1.78
4	<b>ICE</b>	<b>ST</b>	concat	0.69	9.63	1.79
5	<b>ICE</b>	<b>ST</b>	<b>GA</b>	<b>0.66</b>	<b>8.58</b>	<b>1.68</b>

context encoder to extract spatiotemporal context features, in place of single-modality features. Previous studies have typically extracted either temporal context features from event voxels or spatial context features from images. To investigate the differences between these context features, we replace the

fused spatiotemporal features with frame context features and event context features, respectively. For fair comparison, the spatiotemporal features output by MFCE are dimensionally matched to the single-modality features. As shown in rows 3 and 5 of Table IV, extracting context features solely from events results in reduced accuracy (EPE increases from 0.66 to 0.68), highlighting the advantage of spatiotemporal features over event-only features. In row 2, following the typical settings of frame-based optical flow methods, we extract context features exclusively from the first frame. Compared to spatiotemporal features, spatial features lead to a notable drop in accuracy (EPE increases from 0.66 to 0.69), likely due to the lack of rich motion cues available in event data. Furthermore, comparing event context features with frame context features reveals that event features outperform frame-based features. This may be attributed to events capturing both motion cues from intermediate processes and the spatial structure of the scene.

To further validate the effectiveness, we conducted a qualitative comparison. As shown in Fig. 7, the single modality context feature is limited in information, leading to blurred boundaries between the guardrail and background. In contrast, the spatiotemporal context feature delivers clearer boundary predictions by leveraging complementary modalities. In conclusion, although both types of features could provide context information during the iterative refinement process, event-based context features typically yield better performance. The spatiotemporal context features further enhance this by offering more comprehensive information and compact representations.

**Cross-Modal Guided Aggregation.** To enhance inter-modal interactions and achieve a deeper fusion of events and frames, we proposed a cross-modal guided aggregation strategy. Unlike BFlow, which concatenates motion features from both modalities directly, our approach leverages the spatial stability of ICE motion features to guide the aggregation of temporally-dense event motion features. The aggregation module is built on a transformer architecture, where ICE features serve as keys and values to guide and enrich the spatially sparse event motion features. In the ablation study, we replace guided aggregation with direct concatenation for comparison. As shown in rows 4 and 5 of Table IV, the guided aggregation strategy significantly improves the accuracy, confirming that enhancing inter-modal interactions improves modality fusion compared to simple concatenation.

To further validate its effectiveness, we present a qualitative comparison. As illustrated in Fig. 7, while spatiotemporal context features help delineate the boundaries between the foreground and background, background motion shows prediction errors caused by occlusion from the guardrail. Our proposed method mitigates these errors through stable ICE guidance, demonstrating the effectiveness of the guided fusion strategy.

### E. Efficiency

We present the inference time and performance of different approaches in Table V. For correlation-based methods, inference time is significantly affected by the number

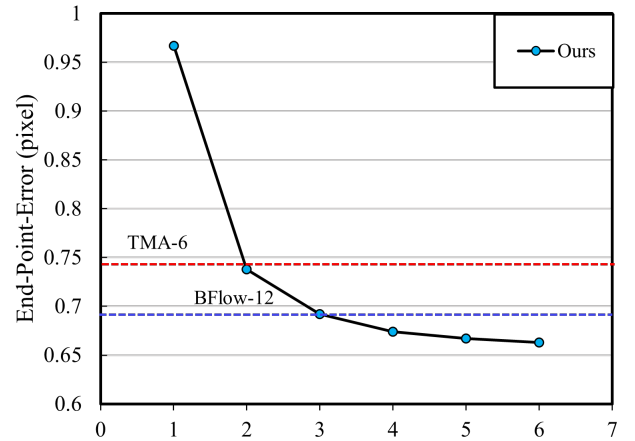


Fig. 8: **EPE vs. Number of iterations at inference.** The figure illustrates prediction accuracy across iterations during inference. Our method exceeds the accuracy of TMA-6 in just two iterations and achieves the accuracy of BFlow-12 in only three iterations, where ‘-N’ indicates the number of iterations.

TABLE V: Comparison of the Computational Performance of Several Iterative Methods.

Methods	Params	Inference time(ms)	iterations	EPE
ERAFT [26]	5.3M	74	12	0.79
TMA [22]	6.9M	43	6	0.74
BFlow [23]	6.5M	111	12	0.69
Ours	9.2M	61	6	0.66

of iterations [52]. As shown in the table, inference time consistently increases with the number of iterations across different methods, revealing a clear trade-off between speed and accuracy. Reducing iterations accelerates inference but leads to a notable drop in accuracy. Our approach addresses this by enhancing the quality of extracted features, enabling higher accuracy with fewer iterations.

We first compare the inference time of our method with TMA to evaluate the overhead from incorporating additional modalities. With the same number of iterations, incorporating new modalities increases inference time by just 18 ms compared to TMA. Despite the slight increase in inference time, the 10% accuracy gain over TMA makes the introduction of new modalities highly beneficial. Next, we compare inference time with other cross-modal methods to assess the efficiency of different fusion strategies. Our method outperforms the state-of-the-art fusion-based method [23] with only half the number of iterations (6 vs. 12), indicating that our aggregated features encode richer and more precise motion cues for refinement. Our method reduces inference time by 45% and lowers end-point error by 4% compared to BFlow. Overall, our approach delivers superior performance in the early iterations. As shown in Fig. 8, our method surpasses the accuracy of TMA-6 at the second iteration and achieves the accuracy of BFlow-12 by the third iteration.

## VI. CONCLUSION AND LIMITATION

This paper explores the fusion of event and frame data for optical flow estimation, leveraging the complementary strengths of both modalities. Our approach integrates the spatial stability of frames with the high temporal resolution of events, introducing a novel paradigm for robust optical flow estimation. Specifically, we reorganize the two modalities into a spatially robust guiding modality, extracting stable features to guide the aggregation of temporally-dense event features. The aggregation module leverages transformer architectures, where guided features are used to enrich event features and guide the temporal aggregation. The proposed guidance strategy enhances cross-modal interactions and fully exploits the complementary strengths between events and frames, enabling more effective fusion. Additionally, we analyze the impact of different contexts in optical flow estimation and introduce a compact spatiotemporal context to replace single-modality contexts. Experimental results demonstrate that our fusion strategy achieves rapid convergence and state-of-the-art accuracy with minimal iterations. Comprehensive ablation studies further validate the robustness and effectiveness of our method.

## REFERENCES

- [1] Zachary Teed and Jia Deng. Raft: Recurrent all-pairs field transforms for optical flow. In *Computer Vision–ECCV 2020: 16th European Conference, Glasgow, UK, August 23–28, 2020, Proceedings, Part II 16*, pages 402–419. Springer, 2020.
- [2] Shihao Jiang, Dylan Campbell, Yao Lu, Hongdong Li, and Richard Hartley. Learning to estimate hidden motions with global motion aggregation. In *Proceedings of the IEEE/CVF International Conference on Computer Vision*, pages 9772–9781, 2021.
- [3] Guillermo Gallego, Tobi Delbrück, Garrick Orchard, Chiara Bartolozzi, Brian Taba, Andrea Censi, Stefan Leutenegger, Andrew J Davison, Jörg Conrath, Kostas Daniilidis, et al. Event-based vision: A survey. *IEEE Transactions on Pattern Analysis and Machine Intelligence*, 44(1):154–180, 2020.
- [4] Zhiwen Chen, Zhiyu Zhu, Yifan Zhang, Junhui Hou, Guangming Shi, and Jinjian Wu. Segment any event streams via weighted adaptation of pivotal tokens. In *Proceedings of the IEEE/CVF Conference on Computer Vision and Pattern Recognition*, pages 3890–3900, 2024.
- [5] Song Wu, Zhiyu Zhu, Junhui Hou, Guangming Shi, and Jinjian Wu. E-motion: Future motion simulation via event sequence diffusion. In *Advances in Neural Information Processing Systems*, 2024.
- [6] Saizhe Ding, Jinze Chen, Yang Wang, Yu Kang, Weiguo Song, Jie Cheng, and Yang Cao. E-mlb: Multilevel benchmark for event-based camera denoising. *IEEE Transactions on Multimedia*, 26:65–76, 2023.
- [7] Yongjian Deng, Hao Chen, and Youfu Li. A dynamic gen with cross-representation distillation for event-based learning. In *Proceedings of the AAAI Conference on Artificial Intelligence*, pages 1492–1500, 2024.
- [8] Bowen Yao, Yongjian Deng, Yuhao Liu, Hao Chen, Youfu Li, and Zhen Yang. Sam-event-adaptor: Adapting segment anything model for event-rgb semantic segmentation. In *2024 IEEE International Conference on Robotics and Automation (ICRA)*, pages 9093–9100. IEEE, 2024.
- [9] Yu Jiang, Yuehang Wang, Siqi Li, Yongji Zhang, Minghao Zhao, and Yue Gao. Event-based low-illumination image enhancement. *IEEE Transactions on Multimedia*, 2023.
- [10] Lin Zhu, Xianzhang Chen, Lizhi Wang, Xiao Wang, Yonghong Tian, and Hua Huang. Continuous-time object segmentation using high temporal resolution event camera. *IEEE Transactions on Pattern Analysis and Machine Intelligence*, 2024.
- [11] Fang Xu, Lei Yu, Bishan Wang, Wen Yang, Gui-Song Xia, Xu Jia, Zhendong Qiao, and Jianzhuang Liu. Motion deblurring with real events. In *Proceedings of the IEEE/CVF International Conference on Computer Vision*, pages 2583–2592, 2021.
- [12] Kang Chen and Lei Yu. Motion deblur by learning residual from events. *IEEE Transactions on Multimedia*, 2024.
- [13] Haoyu Chen, Minggui Teng, Boxin Shi, Yizhou Wang, and Tiejun Huang. A residual learning approach to deblur and generate high frame rate video with an event camera. *IEEE Transactions on Multimedia*, 25:5826–5839, 2022.
- [14] Chu Zhou, Minggui Teng, Jin Han, Jinxiu Liang, Chao Xu, Gang Cao, and Boxin Shi. Deblurring low-light images with events. *International Journal of Computer Vision*, 131(5):1284–1298, 2023.
- [15] Zhiwen Chen, Jinjian Wu, Junhui Hou, Leida Li, Weisheng Dong, and Guangming Shi. Ecsnet: Spatio-temporal feature learning for event camera. *IEEE Transactions on Circuits and Systems for Video Technology*, 33(2):701–712, 2022.
- [16] Zhiyu Zhu, Junhui Hou, and Xianqiang Lyu. Learning graph-embedded key-event back-tracing for object tracking in event clouds. *Advances in Neural Information Processing Systems*, 35:7462–7476, 2022.
- [17] Federico Paredes-Vallés and Guido CHE De Croon. Back to event basics: Self-supervised learning of image reconstruction for event cameras via photometric constancy. In *Proceedings of the IEEE/CVF Conference on Computer Vision and Pattern Recognition*, pages 3446–3455, 2021.
- [18] Yuhao Liu, Yongjian Deng, Hao Chen, and Zhen Yang. Video frame interpolation via direct synthesis with the event-based reference. In *Proceedings of the IEEE/CVF Conference on Computer Vision and Pattern Recognition*, pages 8477–8487, 2024.
- [19] Chao Ding, Mingyuan Lin, Haijian Zhang, Jianzhuang Liu, and Lei Yu. Video frame interpolation with stereo event and intensity cameras. *IEEE Transactions on Multimedia*, 2024.
- [20] Lin Zhu, Yunlong Zheng, Yijun Zhang, Xiao Wang, Lizhi Wang, and Hua Huang. Temporal residual guided diffusion framework for event-driven video reconstruction. In *European Conference on Computer Vision*, pages 411–427. Springer, 2025.
- [21] Yixin Yang, Jinxiu Liang, Bohan Yu, Yan Chen, Jimmy S Ren, and Boxin Shi. Latency correction for event-guided deblurring and frame interpolation. In *Proceedings of the IEEE/CVF Conference on Computer Vision and Pattern Recognition*, pages 24977–24986, 2024.
- [22] Haotian Liu, Guang Chen, Sanqing Qu, Yanping Zhang, Zhijun Li, Alois Knoll, and Changjun Jiang. Tma: Temporal motion aggregation for event-based optical flow. In *Proceedings of the IEEE/CVF International Conference on Computer Vision*, pages 9685–9694, 2023.
- [23] Mathias Gehrig, Manasi Muglikar, and Davide Scaramuzza. Dense continuous-time optical flow from event cameras. *IEEE Transactions on Pattern Analysis and Machine Intelligence*, 2024.
- [24] Lei Sun, Kailun Yang, Xinxin Hu, Weijian Hu, and Kaiwei Wang. Real-time fusion network for rgb-d semantic segmentation incorporating unexpected obstacle detection for road-driving images. *IEEE Robotics and Automation Letters*, 5(4):5558–5565, 2020.
- [25] Zhexiong Wan, Yuchao Dai, and Yuxin Mao. Learning dense and continuous optical flow from an event camera. *IEEE Transactions on Image Processing*, 31:7237–7251, 2022.
- [26] Mathias Gehrig, Mario Millhäusler, Daniel Gehrig, and Davide Scaramuzza. E-raft: Dense optical flow from event cameras. In *2021 International Conference on 3D Vision (3DV)*, pages 197–206. IEEE, 2021.
- [27] Alexey Dosovitskiy, Philipp Fischer, Eddy Ilg, Philip Hausser, Caner Hazirbas, Vladimir Golkov, Patrick Van Der Smagt, Daniel Cremers, and Thomas Brox. FlowNet: Learning optical flow with convolutional networks. In *Proceedings of the IEEE International Conference on Computer Vision*, pages 2758–2766, 2015.
- [28] Deqing Sun, Xiaodong Yang, Ming-Yu Liu, and Jan Kautz. Pwc-net: Cnns for optical flow using pyramid, warping, and cost volume. In *Proceedings of the IEEE Conference on Computer Vision and Pattern Recognition*, pages 8934–8943, 2018.
- [29] Tak-Wai Hui, Xiaoou Tang, and Chen Change Loy. LiteflowNet: A lightweight convolutional neural network for optical flow estimation. In *Proceedings of the IEEE Conference on Computer Vision and Pattern Recognition*, pages 8981–8989, 2018.
- [30] Haofei Xu, Jing Zhang, Jianfei Cai, Hamid Rezaatofighi, and Dacheng Tao. Gmflow: Learning optical flow via global matching. In *Proceedings of the IEEE/CVF Conference on Computer Vision and Pattern Recognition*, pages 8121–8130, 2022.
- [31] Elias Mueggler, Christian Forster, Nathan Baumli, Guillermo Gallego, and Davide Scaramuzza. Lifetime estimation of events from dynamic vision sensors. In *2015 IEEE International Conference on Robotics and Automation (ICRA)*, pages 4874–4881. IEEE, 2015.
- [32] Liyuan Pan, Miaomiao Liu, and Richard Hartley. Single image optical flow estimation with an event camera. In *2020 IEEE/CVF Conference on Computer Vision and Pattern Recognition (CVPR)*, pages 1669–1678. IEEE, 2020.

- [33] Patrick Bardow, Andrew J Davison, and Stefan Leutenegger. Simultaneous optical flow and intensity estimation from an event camera. In *Proceedings of the IEEE Conference on Computer Vision and Pattern Recognition*, pages 884–892, 2016.
- [34] Shintaro Shiba, Yoshimitsu Aoki, and Guillermo Gallego. Secrets of event-based optical flow. In *European Conference on Computer Vision*, pages 628–645. Springer, 2022.
- [35] Alex Zihao Zhu, Liangzhe Yuan, Kenneth Chaney, and Kostas Daniilidis. Ev-flownet: Self-supervised optical flow estimation for event-based cameras. *arXiv preprint arXiv:1802.06898*, 2018.
- [36] Jesse Hagenaaars, Federico Paredes-Vallés, and Guido De Croon. Self-supervised learning of event-based optical flow with spiking neural networks. *Advances in Neural Information Processing Systems*, 34:7167–7179, 2021.
- [37] Guillermo Gallego, Henri Rebecq, and Davide Scaramuzza. A unifying contrast maximization framework for event cameras, with applications to motion, depth, and optical flow estimation. In *Proceedings of the IEEE Conference on Computer Vision and Pattern Recognition*, pages 3867–3876, 2018.
- [38] Federico Paredes-Vallés, Kirk YW Scheper, Christophe De Wagter, and Guido CHE De Croon. Taming contrast maximization for learning sequential, low-latency, event-based optical flow. In *Proceedings of the IEEE/CVF International Conference on Computer Vision*, pages 9695–9705, 2023.
- [39] Jiaming Zhang, Huayao Liu, Kailun Yang, Xinxin Hu, Ruiping Liu, and Rainer Stiefelhagen. Cmx: Cross-modal fusion for rgb-x semantic segmentation with transformers. *IEEE Transactions on Intelligent Transportation Systems*, 2023.
- [40] Bochen Xie, Yongjian Deng, Zhanpeng Shao, and Youfu Li. Eisnet: A multi-modal fusion network for semantic segmentation with events and images. *IEEE Transactions on Multimedia*, 2024.
- [41] Jianping Jiang, Xinyu Zhou, Peiqi Duan, and Boxin Shi. Evplug: Learn a plug-and-play module for event and image fusion. *arXiv preprint arXiv:2312.16933*, 2023.
- [42] Mohammad Mostafavi, Kuk-Jin Yoon, and Jonghyun Choi. Event-intensity stereo: Estimating depth by the best of both worlds. In *Proceedings of the IEEE/CVF International Conference on Computer Vision*, pages 4258–4267, 2021.
- [43] Daniel Gehrig, Michelle Rüegg, Mathias Gehrig, Javier Hidalgo-Carrió, and Davide Scaramuzza. Combining events and frames using recurrent asynchronous multimodal networks for monocular depth prediction. *IEEE Robotics and Automation Letters*, 6(2):2822–2829, 2021.
- [44] Hoonhee Cho and Kuk-Jin Yoon. Selection and cross similarity for event-image deep stereo. In *European Conference on Computer Vision*, pages 470–486. Springer, 2022.
- [45] Zhiyu Zhu, Junhui Hou, and Dapeng Oliver Wu. Cross-modal orthogonal high-rank augmentation for rgb-event transformer-trackers. In *Proceedings of the IEEE/CVF International Conference on Computer Vision*, pages 22045–22055, 2023.
- [46] Zhiwen Chen, Jinjian Wu, Weisheng Dong, Leida Li, and Guangming Shi. Crossei: Boosting motion-oriented object tracking with an event camera. *IEEE Transactions on Image Processing*, 2024.
- [47] Enze Xie, Wenhai Wang, Zhiding Yu, Anima Anandkumar, Jose M Alvarez, and Ping Luo. Segformer: Simple and efficient design for semantic segmentation with transformers. *Advances in Neural Information Processing Systems*, 34:12077–12090, 2021.
- [48] Alex Zihao Zhu, Dinesh Thakur, Tolga Özaslan, Bernd Pfrommer, Vijay Kumar, and Kostas Daniilidis. The multivehicle stereo event camera dataset: An event camera dataset for 3d perception. *IEEE Robotics and Automation Letters*, 3(3):2032–2039, 2018.
- [49] Mathias Gehrig, Willem Aarents, Daniel Gehrig, and Davide Scaramuzza. Dsec: A stereo event camera dataset for driving scenarios. *IEEE Robotics and Automation Letters*, 6(3):4947–4954, 2021.
- [50] Yan Yang, Liyuan Pan, and Liu Liu. Event camera data dense pre-training. In *European Conference on Computer Vision*, pages 292–310. Springer, 2025.
- [51] Yilun Wu, Federico Paredes-Vallés, and Guido CHE De Croon. Lightweight event-based optical flow estimation via iterative deblurring. In *2024 IEEE International Conference on Robotics and Automation (ICRA)*, pages 14708–14715. IEEE, 2024.
- [52] Changxing Deng, Ao Luo, Haibin Huang, Shaodan Ma, Jiangyu Liu, and Shuaicheng Liu. Explicit motion disentangling for efficient optical flow estimation. In *Proceedings of the IEEE/CVF International Conference on Computer Vision*, pages 9521–9530, 2023.